TRI-PP-07-25

Bridging over p-wave π-production and weak processes in few-nucleon systems with chiral perturbation theory

Satoshi X. Nakamura[1,*]

[1] *Theory Group, TRIUMF, 4004 Wesbrook Mall, Vancouver, BC V6T 2A3, Canada*

(Dated: May 14, 2008)

Abstract

I study an aspect of chiral perturbation theory (χPT) which enables one to "bridge" different reactions. That is, an operator fixed in one of the reactions can then be used to predict the other. For this purpose, I calculate the partial wave amplitude for the p-wave pion production ($pp \to pn\pi^+$) using the pion production operator from the lowest and the next nonvanishing orders. The operator includes a contact operator whose coupling has been fixed using a matrix element of a low-energy weak process ($pp \to de^+\nu_e$). I find that this operator does not reproduce the partial wave amplitude extracted from experimental data, showing that the bridging over the reactions with significantly different kinematics is not necessarily successful. I study the dependence of the amplitude on the various inputs such as the NN potential, the $\pi N\Delta$ coupling, and the cutoff. I argue the importance of a higher order calculation. In order to gain an insight into a higher order calculation, I add a higher order counter term to the operator used above, and fit the couplings to both the low-energy weak process and the pion production. The energy dependence of the partial wave amplitude for the pion production is described by the operator consistently with the data. However, I find a result which tells us to be careful about the convergence of the chiral expansion for the $pp \to pn\pi^+$ reaction.

PACS numbers: 25.10.+s, 11.30.Rd, 13.60.Le, 25.40.-h

Keywords: chiral perturbation theory, pion production

*Electronic address: snakamura@triumf.ca

I. INTRODUCTION

Applications of the chiral perturbation theory (χPT) to few-nucleon systems have been of great interest in the last decade. For reviews, see, *e.g.*, Refs. [1]. Particularly, a comprehensive review for the π production is given in Ref. [2], and for the electroweak processes in Ref. [3]. A powerful aspect of χPT is that it provides us with a bridge between different reactions in a model-independent way. This means that coupling constants (the so-called low-energy constants, LECs) fixed using experimental data for one of the reactions can then be used in the other. An interesting interaction in this context is

$$\mathcal{L} = -2d_1 N^\dagger S \cdot u N N^\dagger N \ , \tag{1}$$

with

$$f_\pi u_\mu = -\tau_a \partial_\mu \pi_a - \epsilon_{3ab} V_\mu \pi_a \tau_b + f_\pi A_\mu + \cdots . \tag{2}$$

The spin operator is S, and the external vector (axial) current is V_μ (A_μ). The constant d_1 is a LEC. This contact interaction between the nucleons contributes to the three-nucleon force[4], the p-wave π-production ($pp \to pn\pi^+$[5], $pp \to d\pi^+$), the radiative pion capture on the deuteron ($\pi^- d \to \gamma nn$)[6, 7], and the weak processes in few-nucleon systems, such as tritium β-decay and the proton-proton fusion ($pp \to de^+\nu_e$)[8], the neutrino-induced disintegration of the deuteron ($\nu_e d \to e^- pp$, $\nu d \to \nu pn$)[9], and the muon capture by the deuteron ($\mu^- d \to \nu_\mu nn$)[10]. The contact term in Eq. (1) makes the connection among these reactions, which may be referred to as the two-body analog of the Goldberger-Treiman relation, as stated in Ref. [6]. If all couplings except for d_1 have been fixed using experimental data for πN and NN elastic scattering, then one can fix d_1 using one of the above reactions, and predict the others.

There have been several such calculations which I will refer to as the "bridging program". One of them was done by Park *et al.* [8], where they fixed d_1 using the experimental tritium β-decay rate, and calculated, with no free parameters, the weak proton capture by a proton (or ^{3}He). In this case, all the reactions are low-energy weak processes, and the kinematics are relatively similar. Therefore, the bridging program is expected to work well. In another work due to Hanhart *et al.* [5], the authors calculated the partial wave amplitude for the p-wave π-production ($pp \to pn\pi^+$), and showed that the use of d_1 fixed by three-nucleon observables [4] also consistently reproduces the partial wave amplitude extracted from experimental data [11]. Although this result seems to be satisfactory, the bridging program in this work was not done fully consistently. This is because they used a nuclear force [12] which is different from the nuclear force used for fixing d_1 in Ref. [4]. Because of the short-range nature of the d_1 term, the d_1 value is largely dependent on the choice of the nuclear force. Hanhart *et al.* also showed that the p-wave π-production amplitude is rather largely

dependent on the contribution from the d_1 term. This indicates the importance of careful treatment of the d_1 term in the calculation; the nuclear force and the d_1 value have to be consistent. Finally, I mention the bridging program done by Gårdestig *et al.* [6], where they fixed the d_1 value using the matrix element of $pp \to de^+\nu_e$ and then used it in calculating observables for $\pi^- d \to \gamma nn$. The two reactions are similar in kinematics of the NN sector, but are rather different in the momentum transfer, which might have to be taken care of. They are interested in extracting the neutron-neutron scattering length from the $\pi^- d \to \gamma nn$ reaction and, for that purpose, they are interested in the shape of the spectrum rather than the absolute value. They found that the use of the d_1 term fixed in the above manner significantly reduces the dependence of the shape on R which is the matching point between the long range one-pion-exchange potential and the short range square well potential. Although this result is a success of the bridging program, it is still interesting to study the absolute value of the cross section in order to more rigorously test the power of χPT.

In this work, I would like to more seriously investigate how reliably the bridging program, an important aspect of χPT, works. I believe that my investigation is important because there has been sometimes an argument which supposes that the bridging program works, even though it has not been quantitatively confirmed that a bridging program over reactions with considerably different kinematics works. For this purpose, I calculate the partial wave amplitude for the p-wave π-production in NN collision ($pp \to pn\pi^+$), with d_1 fixed by an observable of a low-energy weak process. This obviously provides a stringent test of χPT, because the two reactions are strong and weak processes, and are quite different in kinematics. My program is as follows. I extend the operator of Ref. [8] by including the Δ, which is known to play an important role in the p-wave π-production, and re-fit d_1 to an observable of a weak process. Here, I fit d_1 to a matrix element of the axial vector current used in Ref. [8]: the kinematics is that for the $pp \to de^+\nu_e$ reaction. The π-production operators I use are the same as those used in Ref. [5], except that the Δ is treated differently. In Ref. [5], a coupled-channel equation was solved and the Δ is included in the nuclear wave functions [12]. I use nuclear wave functions including only the nucleons as dynamical degrees of freedom. I take account of the Δ by including it in the π-production operator. [1] The π-production operator I use is based on a counting rule proposed in Ref. [5, 13], which is different from Weinberg's counting[14], and the large initial on-shell momentum [$\sim \sqrt{m_N m_\pi}$, m_N (m_π) : the nucleon (pion) mass] is considered as a characteristic scale of the system. I consider the operators up to next-to-leading order [NLO, $\mathcal{O}(m_\pi/m_N)$]. [2]

[1] Thus I treat the Δ perturbatively and do not fully take account of some non-perturbative effect of the Δ in wave functions. A calculation with a fuller account of the Δ might be worthwhile doing to see a difference.

[2] The operator used in Ref. [8] is based on Weinberg's counting while the operator used in Ref. [5] is based on the counting proposed in Ref. [5, 13]. Therefore, one may wonder whether the two operators contain

It is very interesting to see whether the operator constructed using the low-energy weak process can reasonably describe the π production. I will use several combinations of the inputs (the $\pi N\Delta$ coupling, the NN potential, cutoff) in my calculation. Even though the d_1 value is fixed for each combination of the inputs so that the low-energy weak process is reproduced, one may expect a dependence of the π production amplitude on the combination because of the rather different kinematics between the two reactions. I will study such a dependence. In fact, we will see that this bridging program is not successful when working with the NLO operators; the partial wave amplitude of the π production based on χPT is not consistent with the data. I will argue the importance of going to a higher order calculation. In order to, even roughly, explore a result of a higher order calculation, I add a higher order counter term and study a consequence.

This paper is organized as follows. In Sec. II, I present the chiral operator for the p-wave π-production up to the order I work with. I discuss the determination of the d_1 value using the low-energy weak process in Sec. III. In Sec. IV, I perform a multipole expansion of the operator, and express the cross section in terms of the partial wave amplitudes. Then, in Sec. V, I present my result for the p-wave π production amplitudes and compare them with the data. The result obtained with the higher order counter term is also presented. Finally I summarize this work in Sec. VI.

II. CHIRAL OPERATOR FOR p-WAVE π-PRODUCTION

I present expressions of chiral operators which contribute to the p-wave π-production. I basically follow Ref. [5], except for the treatment of the Δ degree of freedom, and the way how the high momentum components are cut off. I start with the chiral interaction Lagrangian given in Ref. [15]. By keeping terms relevant to my calculation, I have

$$\begin{aligned}\mathcal{L}^{(0)}_{\rm int} \;=\; & -\frac{1}{4f_\pi^2}N^\dagger \boldsymbol{\tau}\cdot(\boldsymbol{\pi}\times\dot{\boldsymbol{\pi}})N + \frac{g_A}{2f_\pi}N^\dagger(\boldsymbol{\tau}\vec{\sigma}\cdot\vec{\nabla}\boldsymbol{\pi})N \\ & + \frac{h_A}{2f_\pi}N^\dagger(\boldsymbol{T}\vec{S}\cdot\vec{\nabla}\boldsymbol{\pi})\Delta + \text{h.c.}\,, \end{aligned} \tag{3}$$

and

$$\begin{aligned}\mathcal{L}^{(1)}_{\rm int} = & \frac{i}{8m_N f_\pi^2}N^\dagger\boldsymbol{\tau}\cdot(\boldsymbol{\pi}\times\vec{\nabla}\boldsymbol{\pi})\cdot\vec{\nabla}N - \frac{c_3}{f_\pi^2}N^\dagger(\vec{\nabla}\boldsymbol{\pi})^2 N \\ & -N^\dagger\frac{\bar{c}_4}{2f_\pi^2}\vec{\sigma}\cdot\vec{\nabla}\boldsymbol{\pi}\times\vec{\nabla}\boldsymbol{\pi}\cdot\boldsymbol{\tau}N - \frac{ig_A}{4m_N f_\pi}N^\dagger\boldsymbol{\tau}\cdot\dot{\boldsymbol{\pi}}\vec{\sigma}\cdot\vec{\nabla}N \\ & -\frac{ih_A}{4m_N f_\pi}N^\dagger\boldsymbol{T}\cdot\dot{\boldsymbol{\pi}}\vec{S}\cdot\vec{\nabla}\Delta - \frac{d_1}{f_\pi}N^\dagger\boldsymbol{\tau}\vec{\sigma}\cdot\vec{\nabla}\boldsymbol{\pi}N\,N^\dagger N\end{aligned}$$

different mechanisms and thus the d_1 value is different in each case. I will argue in Sec. III that the d_1 value should be the same in the both cases, up to the order I am working.

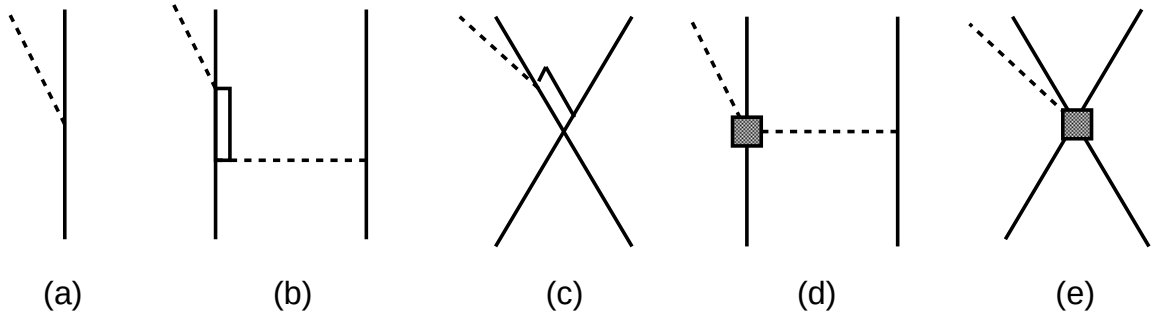

FIG. 1: The p-wave π-production operators up to NLO in χPT. Dashed lines denote pions and the solid lines nucleons, the double lines Δ. Vertices without (with) the shaded box arise from the leading (subleading) order Lagrangian.

$$-\frac{d_2}{2f_\pi}\vec{\nabla}\boldsymbol{\pi}\times N^\dagger\vec{\sigma}\boldsymbol{\tau}N\ \cdot N^\dagger\vec{\sigma}\boldsymbol{\tau}N+\text{h.c.}, \tag{4}$$

with $\bar{c}_4 = c_4 + \frac{1}{4m_N}$. The nucleon's spin (isospin) operator is $\vec{\sigma}$ ($\boldsymbol{\tau}$), while the $N\Delta$ transition spin (isospin) operator is $\vec{S}$ ($\boldsymbol{T}$). I use the pion decay constant $f_\pi = 93$ MeV and the nucleon mass, $m_N = 939$ MeV. Regarding the parameters (g_A, h_A, c_3, c_4), I follow Ref. [16], where Krebs *et al.* constructed a chiral nuclear force including the Δ explicitly. The axial coupling constant is g_A $(= 1.27)$. For the $\pi N\Delta$ coupling, I use two choices: $h_A = 2.10$ from the Δ-decay width[17], and $h_A = 3g_A/\sqrt{2} = 2.68$ from large N_C. [3] In Ref. [16], the authors calculated the s- and p-wave πN scattering threshold parameters at next-to-leading order with taking account of the Δ, and fit the couplings (c_3, c_4 and others) to the analysis of Matsinos[18]. The result is $c_3 = -1.87$ GeV^{-1}, $c_4 = 1.87$ GeV^{-1} for $h_A = 2.10$, and $c_3 = -0.79$ GeV^{-1}, $c_4 = 1.33$ GeV^{-1} for $h_A = 2.68$. The remaining unknown LECs are d_1 and d_2 which will be determined in the next section.

I use the following π-production operator derived from the above interaction Lagrangian. The leading order [LO, $\mathcal{O}(1)$] operator is the one-body direct production of the pion with the isospin state a off the nucleon [Fig. 1(a)],

$$O_{\rm 1B} \ = \ i\frac{g_A}{2f_\pi}(2\pi)^3\delta^{(3)}(\boldsymbol{p}_2'-\boldsymbol{p}_2)\tau_1^a\boldsymbol{\sigma}_1\cdot\boldsymbol{q}_\pi \ + \ (1\leftrightarrow 2)\ , \tag{5}$$

where $\boldsymbol{q}_\pi$ is the momentum of the emitted pion. The quantity $\boldsymbol{p}_i$ ($\boldsymbol{p}_i'$) is the momentum of the incoming (outgoing) i-th nucleon. Another LO mechanism I consider is the Δ-excitation followed by the π emission. In Ref. [5], the authors used the wave function which explicitly includes the Δ component, and considered the one-body operator which produces the pion with the Δ deexcited to the nucleon. Because I use nuclear wave functions with only

[3] The definition of the $\pi N\Delta$ coupling constant here is different from that of Ref. [16] by a factor of 2: h_A (this work) $= 2h_A$ (Ref. [16]).

the nucleonic degrees of freedom, I alternatively use a two-body operator in which the Δ is excited either by the π-exchange [Fig. 1(b)], or by a contact interaction between the nucleons [Fig. 1(c)]. The former is given by

$$O_{\Delta\pi} \;=\; \frac{i}{36}\,\frac{g_A h_A^2}{f_\pi^3}\,\frac{\boldsymbol{\sigma}_2\cdot\boldsymbol{k}}{m_\pi'^2+k^2}\,\frac{(4\tau_2^a\boldsymbol{k}-(\boldsymbol{\tau}_1\times\boldsymbol{\tau}_2)^a\boldsymbol{\sigma}_1\times\boldsymbol{k}\,)\cdot\boldsymbol{q}_\pi}{m_\Delta-m_N-p_o^2/m_N+(\boldsymbol{p}'+\boldsymbol{q}_\pi/2)^2/2\mu}\;+\;(1\leftrightarrow 2)\;, \quad (6)$$

where m_Δ (= 1232 MeV) is the mass of the Δ, and p_o is the initial on-shell relative NN momentum. The quantities, μ, k, p' are respectively defined by $\mu \equiv m_N m_\Delta/(m_N+m_\Delta)$, $\boldsymbol{k}\equiv\boldsymbol{p}_2-\boldsymbol{p}_2'$ and $\boldsymbol{p}'\equiv(\boldsymbol{p}_1'-\boldsymbol{p}_2')/2$. I assume the equal energy sharing between the nucleons and $m_\pi'^2\equiv(3m_\pi^2-q_\pi^2)/4$, m_π = 138 MeV. In Appendix, I explain how I treat the energy denominator in Eq. (6) in my calculation. An expression for the diagram in Fig. 1(c) is

$$O_{\Delta\rm CT} \;=\; -\frac{i}{9}\,\frac{h_A C_2^{N\Delta}}{f_\pi}\,\frac{(4\,\tau_2^a\,(\boldsymbol{\sigma}_2\times\boldsymbol{k})\times\boldsymbol{k}_j-(\boldsymbol{\tau}_1\times\boldsymbol{\tau}_2)^a\,\boldsymbol{\sigma}_1\times[(\boldsymbol{\sigma}_2\times\boldsymbol{k})\times\boldsymbol{k}])\cdot\boldsymbol{q}_\pi}{m_\Delta-m_N-p_o^2/m_N+(\boldsymbol{p}'+\boldsymbol{q}_\pi/2)^2/2\mu}$$
$$+\;(1\leftrightarrow 2)\;, \quad (7)$$

where I have used the contact $NN\to N\Delta$ interaction with two derivatives,

$$\mathcal{L}_{NN\to N\Delta} = -iC_2^{N\Delta}\Delta^\dagger \boldsymbol{T}\left(\vec{S}\cdot(\overrightarrow{\nabla}+\overleftarrow{\nabla})\vec{\sigma}-\vec{S}\vec{\sigma}\cdot(\overrightarrow{\nabla}+\overleftarrow{\nabla})\right)N\cdot N^\dagger\left(\vec{\sigma}\times(\overrightarrow{\nabla}+\overleftarrow{\nabla})\right)\boldsymbol{\tau}N\;. \quad (8)$$

It is noted that a contact $NN\to N\Delta$ interaction without derivative does not contribute to the transition under consideration. I use the $C_2^{N\Delta}$ value taken from the resonance saturation of the ρ-exchange $NN\to N\Delta$ potential used in several phenomenological models[19]:

$$h_A C_2^{N\Delta} \;=\; g_A\frac{18}{25}\,\frac{g_{\rho NN}^2}{m_N^2}\,(1+\kappa_\rho)^2\,\frac{1}{m_\rho^2}\;, \quad (9)$$

where the ρNN vector coupling is $g_{\rho NN}$ ($g_{\rho NN}^2/4\pi$ = 0.5) and the tensor coupling is κ_ρ (= 6.6). The factor at the end, $1/m_\rho^2$ (m_ρ = 770 MeV), is the static limit of the ρ-meson propagator. Although Eq. (8) is not a general contact $NN\to N\Delta$ interaction with two derivatives, one may take account of the most important part of the $NN\to N\Delta$ contact interaction by invoking a meson-exchange model, and the remaining part may be phenomenologically absorbed by the contact d_i ($i=1,2$) terms. Obviously, my treatment of the Δ is rather phenomenological. However, a construction of a nuclear force from a chiral Lagrangian with the π, N and Δ, which is yet to be done [4], is necessary to determine the $C_2^{N\Delta}$ value. I believe that my treatment is one of what one can do best for the moment, and expect a fully consistent calculation in future.

Next I discuss next-to-leading order [NLO, $\mathcal{O}(m_\pi/m_N)$] terms which consist of four types. One of them is the recoil correction to the LO terms. The recoil corrections to the one-body term [Eq. (5)], $\pi\Delta$ term [Eq. (6)], and contact-Δ term [Eq. (7)] are respectively given by

$$O_{\rm 1B,recoil} \;=\; -i\frac{g_A\omega_\pi}{4m_N f_\pi}(2\pi)^3\delta^{(3)}(\boldsymbol{p}_2'-\boldsymbol{p}_2)\tau_1^a\boldsymbol{\sigma}_1\cdot(\boldsymbol{p}_1+\boldsymbol{p}_1')\;+\;(1\leftrightarrow 2)\;, \quad (10)$$

[4] Such a nuclear force for the peripheral wave has been constructed recently [16].

$$O_{\Delta\pi,\mathrm{recoil}} = -\frac{i}{72}\frac{\omega_\pi}{m_N}\frac{g_A h_A^2}{f_\pi^3}\frac{\boldsymbol{\sigma}_2\cdot\boldsymbol{k}}{m_\pi'^2+k^2} \times \frac{4\tau_2^a \boldsymbol{k}\cdot(\boldsymbol{p}_1+\boldsymbol{p}_1') - (\boldsymbol{\tau}_1\times\boldsymbol{\tau}_2)^a\left[(\boldsymbol{\sigma}_1\times\boldsymbol{k})\cdot(\boldsymbol{p}_1+\boldsymbol{p}_1')+2ik^2\right]}{m_\Delta - m_N - p_o^2/m_N + (\boldsymbol{p}'-\boldsymbol{q}_\pi)^2/2\mu} + (1\leftrightarrow 2)\ , \tag{11}$$

$$O_{\Delta\mathrm{CT},\mathrm{recoil}} = \frac{i}{18}\frac{\omega_\pi}{m_N}\frac{h_A C_2^{N\Delta}}{f_\pi}\frac{1}{m_\Delta - m_N - p_o^2/m_N + (\boldsymbol{p}'-\boldsymbol{q}_\pi)^2/2\mu} \times \Big\{\tau_2^a\left[-2k^2\boldsymbol{k}\cdot(\boldsymbol{\sigma}_1\times\boldsymbol{\sigma}_2) + 4((\boldsymbol{\sigma}_2\times\boldsymbol{k})\times\boldsymbol{k})\cdot(\boldsymbol{p}_1+\boldsymbol{p}_1')\right] - (\boldsymbol{\tau}_1\times\boldsymbol{\tau}_2)^a\ (\boldsymbol{\sigma}_1\times((\boldsymbol{\sigma}_2\times\boldsymbol{k})\times\boldsymbol{k}))\cdot(\boldsymbol{p}_1+\boldsymbol{p}_1')\Big\} + (1\leftrightarrow 2)\ , \tag{12}$$

where ω_π is the energy of the emitted pion. The second type of the NLO operator is a pion rescattering through either the c_3 term, or the c_4 term or the Galilean correction to the Weinberg-Tomozawa term [the first term in Eq. (4)]. They are graphically represented by Fig. 1(d), and their expressions are given by

$$O_{c_3} = -i\frac{c_3 g_A}{f_\pi^3}\frac{\boldsymbol{\sigma}_2\cdot\boldsymbol{k}}{m_\pi'^2+k^2}\boldsymbol{k}\cdot\boldsymbol{q}_\pi\tau_2^a + (1\leftrightarrow 2)\ , \tag{13}$$

$$O_{c_4} = -i\frac{\bar{c}_4 g_A}{2f_\pi^3}\frac{\boldsymbol{\sigma}_2\cdot\boldsymbol{k}}{m_\pi'^2+k^2}(\boldsymbol{\sigma}_1\times\boldsymbol{k})\cdot\boldsymbol{q}_\pi(\boldsymbol{\tau}_1\times\boldsymbol{\tau}_2)^a + (1\leftrightarrow 2)\ , \tag{14}$$

$$O_{\mathrm{WT,Galilean}} = \frac{g_A}{16 m_N f_\pi^3}\frac{\boldsymbol{\sigma}_2\cdot\boldsymbol{k}}{m_\pi'^2+k^2}(\boldsymbol{q}_\pi-\boldsymbol{k})\cdot(\boldsymbol{p}_1+\boldsymbol{p}_1')(\boldsymbol{\tau}_1\times\boldsymbol{\tau}_2)^a + (1\leftrightarrow 2)\ . \tag{15}$$

For a convenience, I decompose the last term as $O_{\mathrm{WT,Galilean}} = O_{\mathrm{WT1(G)}} + O_{\mathrm{WT2(G)}}$ with [5]

$$O_{\mathrm{WT1(G)}} = \frac{g_A}{16 m_N f_\pi^3}\frac{\boldsymbol{\sigma}_2\cdot\boldsymbol{k}}{m_\pi'^2+k^2}(2\boldsymbol{p}'+\boldsymbol{k})\cdot\boldsymbol{q}_\pi(\boldsymbol{\tau}_1\times\boldsymbol{\tau}_2)^a + (1\leftrightarrow 2)\ , \tag{16}$$

$$O_{\mathrm{WT2(G)}} = \frac{g_A}{16 m_N f_\pi^3}\frac{\boldsymbol{\sigma}_2\cdot\boldsymbol{k}}{m_\pi'^2+k^2}(-k^2-2\boldsymbol{p}'\cdot\boldsymbol{k})(\boldsymbol{\tau}_1\times\boldsymbol{\tau}_2)^a + (1\leftrightarrow 2)\ . \tag{17}$$

[5] When convoluted with the wave functions, $O_{\mathrm{WT,Galilean}}$ gives a non-vanishing amplitude in the soft pion limit. (The tree amplitude vanishes in the soft pion limit.) This is not consistent with chiral symmetry. This problem is similar to that found in Ref. [20] in the context of the s-wave pion production in the NN collision. The solution to this problem was given in Ref. [21]. Probably, the problem here is also resolved by the same mechanism found in Ref. [21]; e.g., one loop diagram formed by $O_{\mathrm{WT,Galilean}}$ and the one-pion-exchange potential is (partly) canceled out by other irreducible pion loop diagrams, leaving a contribution consistent with the chiral symmetry. One may take some prescription to maintain the chiral symmetry. However, I use Eq. (15) without modification because this term gives a small contribution (a few percents) to an amplitude for the $pp\to pn\pi^+$ reaction; the modification will not significantly change results.

The third type of the NLO terms is a pion rescattering via the Weinberg-Tomozawa term:

$$O_{\rm WT} \ = \ -\frac{3g_A\omega_\pi}{16f_\pi^3}\frac{\boldsymbol{\sigma}_2\cdot\boldsymbol{k}}{m_\pi'^2+k^2}(\boldsymbol{\tau}_1\times\boldsymbol{\tau}_2)^a \ + \ (1\leftrightarrow 2) \ . \tag{18}$$

Finally, the fourth type is a pion emission from the contact terms [the d_1 and d_2 terms in Eq. (4), Fig. 1(e)]:

$$O_d \ = \ -i\left(\frac{d_1}{f_\pi}\boldsymbol{\sigma}_1\tau_1^a+\frac{d_2}{2f_\pi}(\boldsymbol{\sigma}_1\times\boldsymbol{\sigma}_2)(\boldsymbol{\tau}_1\times\boldsymbol{\tau}_2)^a\right)\cdot\boldsymbol{q}_\pi + \ (1\leftrightarrow 2) \ . \tag{19}$$

Starting with the operators presented above, I take the following procedure to obtain the momentum space (p-space) operator contributing to the ${}^1S_0 \to {}^3S_1$-${}^3D_1$ transition. At first, I perform Fourier transformation of the above operators to represent them in the coordinate space (r-space). In the Fourier transformation, I multiply a Gaussian cutoff function, $\exp(-k^2/\Lambda_G^2)$, to the operators other than the one-body operators; I use $\Lambda_G = 2$ GeV. In the r-space, I perform the multipole expansion of the operators, and evaluate the matrix elements for the spin, isospin and angular parts of the operators. The remaining radial part of the operators is converted to the p-space using Fourier transformation, and I obtain the radial part of the p-space operator, $O(p',p)$, where p (p') is off-shell relative momentum of the incoming (outgoing) two nucleons. I classify the operators into two groups:

$$\begin{aligned}&\text{Group I} \ : O_{\Delta\pi},\, O_{\Delta\rm CT},\, O_{c_3} \ , O_{c_4},\, O_d\\ &\text{Group II} : O_{\rm 1B},\, O_{\rm 1B,recoil},\, O_{\Delta\pi,\rm recoil},\, O_{\Delta\rm CT,recoil} \ , O_{\rm WT,Galilean},\, O_{\rm WT}\end{aligned}$$

I introduce a sharp cutoff Λ for the operators belonging to Group I such that

$$\begin{aligned}O_\Lambda(p',p) \ &= \ O(p',p) \ , \qquad \text{for} \ \ p\le\Lambda \ \ \text{and} \ p'\le\Lambda \ ,\\ O_\Lambda(p',p) \ &= \ 0 \ , \qquad\qquad\qquad \text{otherwise} \ .\end{aligned} \tag{20}$$

I do not apply the sharp cutoff to the operators of Group II. As we will see in the next section where the LECs d_i are determined using low-energy weak processes, the renormalization of d_i only takes care of high momentum components (larger than Λ) of the operators in Group I. The LECs d_i contain the same physics for both the reactions bridged. Therefore, I retain the high momentum components of the operators in Group II in my calculation. [6] As representatives, I choose $\Lambda = 500$, 600 and 800 MeV. I use the p-space operator explained above because of its usefulness for the renormalization group (RG) analysis which will be done later.

[6] One may also apply the sharp cutoff to the Group II operators, which amounts to cutting off a higher order effect.

For the purpose of the multipole expansion of the π production operator, which will be done in Sec. IV, I express the above π production operators as follows:

$$O_X \;=\; -\vec{O}_X \cdot \vec{Q}, \qquad X = \text{1B},\ \Delta\pi,\ \Delta\text{CT},\ c_3,\ c_4,\ \text{WT1(G)},\ d \tag{21}$$

$$O_Y \;=\; O_Y^0\ \ Q^0, \qquad Y = \text{recoil terms},\ \text{WT2(G)},\ \text{WT} \tag{22}$$

where $\vec{Q} = i\vec{q}_\pi/2f_\pi$ and $Q^0 = i\omega_\pi/2f_\pi$. I will refer to $\vec{O}_X$ as the spatial component of the π production operator while O_Y^0 as the time component.

III. DETERMINATION OF d_i

In this section, I determine the LECs d_i in Eq. (19) using an observable of a low-energy weak process. The d_i terms contribute to the ${}^1S_0 \to {}^3S_1$ transition and appear as a single linear combination, $\tilde{d} \equiv d_1 + 2d_2$. Because d_1 and d_2 are not separately determined by considering the ${}^1S_0 \to {}^3S_1$ transition only, I determine $\tilde{d}$ rather than d_1 and d_2 individually.

In Ref. [8], the authors fixed $\tilde{d}$ using the experimental data of the tritium β-decay rate. [7] They derived the axial vector current contributing the tritium β-decay from the chiral Lagrangian. They did not explicitly consider the Δ as a degree of freedom. The spatial component of the axial vector currents used in Ref. [8] are obtained from the one-body operator [Eq. (5)] and Group I operators without the Δ [Eqs. (13), (14) and (19)], with the factor of $(i\boldsymbol{q}_\pi/2f_\pi)$ being eliminated and m'_π replaced by m_π. Accordingly, the parameters (c_i) used in Ref. [8] are different from those presented in the previous section. Although they additionally included some other operators which give a negligible contribution, I do not consider them in the following. They multiply a Gaussian cutoff function, $\exp\left(-k^2/\Lambda_\chi^2\right)$, to the operators, with $\Lambda_\chi = 500$, 600 and 800 MeV. For each choice of Λ_χ, they fixed $\tilde{d}$ so that the tritium β-decay rate is reproduced. They used the AV18 NN potential [22] supplemented by the Urbana-IX three-nucleon potential [23] when calculating the matrix element for the tritium β-decay.

Here, I need to re-fit the value of $\tilde{d}$ in "my" axial current operator. My operator is the axial current operator used in Ref. [8] plus the Δ-excitation current. The Δ-excitation current is obtained from Eqs. (6) and (7) by eliminating the factor of $(i\boldsymbol{q}_\pi/2f_\pi)$ and $m'_\pi \to m_\pi$. The way of cutting off the high momentum states is also different from that used in Ref. [8], as has been discussed in the previous section. I do not directly use the tritium β-decay rate but take an indirect way to fix $\tilde{d}$, as discussed in the next paragraph.

I start with a benchmark calculation to which the $\tilde{d}$ value in my operator is fitted. For that purpose, I use the same spatial axial current operator used in Ref. [8] (the same couplings

[7] The authors fixed dimensionless constant $\hat{d}_R$ rather than $\tilde{d}$. The two quantities are related through $\hat{d}_R = (m_N f_\pi^2/g_A)\tilde{d} + \hat{c}_3/3 + 2\hat{c}_4/3 + 1/6$, with $c_{3,4} = \hat{c}_{3,4}/m_N$.

TABLE I: Dimensionless contact coupling, $\hat{d}(\equiv m_N f_\pi^2\ \tilde{d})$. The first column is the sharp cutoff value. The first row specifies the NN potentials used. For each NN potential, the left side is $\hat{d}$ for $h_A = 2.10$, while the right side is for $h_A = 2.68$.

Λ	CD-Bonn		AV18		Reid93		Nij I		N^{3}LO	
500	0.18	0.06	−0.01	−0.17	−0.48	−0.64	0.29	0.15	−0.03	−0.20
600	0.62	0.42	0.77	0.47	0.17	−0.13	0.93	0.67	0.60	0.32
800	1.74	1.32	4.36	3.32	3.16	2.11	2.75	2.13	1.18	0.81

and the same cutoff but without the negligible operators) to calculate a matrix element for the ${}^1S_0 \to {}^3S_1$-${}^3D_1$ transition in two-nucleon system. This matrix element is the benchmark to which $\tilde{d}$ is re-fitted so that "my" operator reproduces the same matrix element. In the benchmark calculation, I use the AV18 potential for consistency, and choose a kinematics with $T^i_{NN} = 0.5$ MeV (T^i_{NN} : the initial on-shell kinetic energy of the relative motion), the deuteron final state, and $q = 2.5$ MeV (q : the momentum transfer from the two-nucleon system to the external current). This kinematics is for the low-energy $pp \to de^+\nu_e$ reaction. I use the proton-neutron interaction to generate the initial wave functions, and therefore do not consider the Coulomb interaction and the isospin violation effect. I calculate the matrix element with different choices of the Gaussian cutoff, $\Lambda_\chi = 500$, 600 and 800 MeV. I average the three matrix elements which have a slight cutoff dependence, and regard the average as the benchmark. When I calculate the matrix element of my operator, I use several combinations of the NN potential, the $\pi N\Delta$ coupling (h_A) and the corresponding c_i values, and the sharp cutoff value (Λ). I use the following NN potentials: the CD-Bonn[24], the AV18[22], the Reid93[25], the Nijmegen I[25] and the chiral N^{3}LO[26] potentials. [8] For each combination of these inputs, the $\tilde{d}$ value is fitted to the benchmark, and the result is given in Table I. In the table, I show the dimensionless coupling $\hat{d}(\equiv m_N f_\pi^2\ \tilde{d})$. Although the $\tilde{d}$ value is adjusted so that the benchmark is reproduced irrespective of changing the inputs, it would be expected that the π-production amplitude, evaluated in a significantly different kinematics, have the dependence on them. I will study the dependence later.

Before closing this section, I discuss the issue mentioned in footnote 2. In order for the bridging program to be meaningful, the $\tilde{d}$ term has to (implicitly) include the same mechanisms (up to the external probe) for both of the reactions bridged. If the $\tilde{d}$ term for one of the reactions includes a mechanism which is explicitly considered in the other, the $\tilde{d}$ value

[8] I take the hybrid approach where a matrix element of the chiral operator is sandwiched by wave functions obtained with a phenomenological nuclear force. This approach is also referred to as more effective effective field theory (MEEFT). An argument for employing MEEFT is given in Ref. [27].

should be different in each case. In the case under consideration, the axial current operator and the pion production operator are based on different counting schemes, and therefore there is a concern that the two operators explicitly contain different mechanisms. In the following, I will argue that the $\tilde{d}$ term includes the same physics for both of the operators, up to the order I am working. As we have seen in the above, all of the mechanisms for the axial vector current are included in the pion production operator (up to the external probe). However, the pion production operator contains some mechanisms which are not included in the axial vector current; the recoil corrections, WT and WT(G). Among them, WT and WT(G) do not contribute to the weak process, and thus the $\tilde{d}$ term fixed in the weak process does not contain these mechanisms. The recoil correction of the one-body axial current [the counterpart of Eq. (10)] has been considered in Ref. [8], which means that the $\tilde{d}$ term fixed in Ref. [8] does not contain this mechanism. Although I did not consider this mechanism when fixing $\tilde{d}$, I am safe because this mechanism gives only a negligible contribution to the matrix element considered. The recoil corrections of the Δ axial current [the counterpart of Eqs. (11) and (12)] have not been considered in Ref. [8]. However, the $\tilde{d}$ value does not depend on the inclusion of these mechanisms because they give a negligible contribution to the matrix element. (In fact, these recoil corrections should be captured by another higher order counter term.) Therefore, up to the order I am working, the $\tilde{d}$ term contains the same physics for both of the reactions bridged, and I can use the $\tilde{d}$ term fixed in this section for calculating the pion production amplitude.

IV. PARTIAL WAVE AMPLITUDE AND CROSS SECTION

In this section, I will express the cross section for the $pp \to pn\pi^+$ reaction in terms of partial wave amplitudes. [9] For this purpose, I perform the standard multipole expansion of the π production operator[28], and a partial wave expansion of the initial and final NN scattering wave functions. Then, I use the partial wave amplitudes to express the transition amplitude, and subsequently the cross section. I perform these expansions in the r-space, which will be followed by the conversion into the p-space.

A. Partial wave amplitude

The multipole operator for the time component of a π production operator is defined by

$$T_C^{JM}(\mathcal{O}) \;=\; \int d\boldsymbol{x} j_J(qx) Y_{JM}(\hat{\boldsymbol{x}}) \mathcal{O}^0(\boldsymbol{x}), \tag{23}$$

[9] I will work with the center-of-mass system of the initial pp system throughout this work.

where $\boldsymbol{q} \equiv -\boldsymbol{q}_\pi$ ($q = |\boldsymbol{q}|$), $j_J(qx)$ is the spherical Bessel function of order J, and $\hat{\boldsymbol{x}} \equiv \boldsymbol{x}/|\boldsymbol{x}|$. An r-space operator is $\mathcal{O}^0(\boldsymbol{x})$, the dependence on the center-of-mass coordinate being eliminated; *e.g.*, $\mathcal{O}^0(\boldsymbol{x}) = O^0(\boldsymbol{x})|_{\boldsymbol{R}=0}$. For the spatial component of the π production operator, I show only the longitudinal multipole operator because the electric and magnetic multipole operators give vanishing contribution for the case in question:

$$T_L^{JM}(\mathcal{O}) \;=\; \frac{i}{q}\int d\boldsymbol{x}\boldsymbol{\nabla}[j_J(qx)Y_{JM}(\hat{\boldsymbol{x}})]\cdot\vec{\mathcal{O}}(\boldsymbol{x}). \tag{24}$$

The transition amplitude for the $pp \to pn\pi^+$ reaction is written by

$$T_{fi} = \langle\psi_f|\int d\boldsymbol{x}\; e^{i\boldsymbol{q}\cdot\boldsymbol{x}}\left[\sum_Y \mathcal{O}_Y^0(\boldsymbol{x})Q^0 - \sum_X \vec{\mathcal{O}}_X(\boldsymbol{x})\cdot\vec{Q}\right]|\psi_i\rangle\;, \tag{25}$$

where ψ_i (ψ_f) is the nuclear wave function for the initial (final) state, whose r-space representation will be given later. In the summations in Eq. (25), X (Y) takes various components of the π production operator specified in Eq. (21) [Eq. (22)]. The four-vector Q has been defined in Eqs. (21) and (22). Using the multipole operators presented above, I can rewrite T_{fi} as

$$T_{fi} \;=\; \sum_{J_oM_o} 4\pi i^{J_o}(-1)^{M_o}\langle\psi_f|\left[T_C^{J_oM_o}Q_C^{J_o-M_o} + T_L^{J_oM_o}Q_L^{J_o-M_o}\right]|\psi_i\rangle\;, \tag{26}$$

with

$$Q_C^{JM} \;=\; Y_{JM}(\hat{\boldsymbol{q}})\;Q^0, \tag{27}$$

$$Q_L^{JM} \;=\; \left(\sqrt{\frac{J}{2J+1}}\boldsymbol{Y}_{J-1JM}(\hat{\boldsymbol{q}}) - \sqrt{\frac{J+1}{2J+1}}\boldsymbol{Y}_{J+1JM}(\hat{\boldsymbol{q}})\right)\cdot\boldsymbol{Q}\;, \tag{28}$$

and $\boldsymbol{Y}_{JLM}(\hat{\boldsymbol{q}})$ are the vector spherical harmonics.

Now I proceed to the partial wave expansion of the NN wave function. An NN scattering wave function with the relative momentum $\boldsymbol{p}$, the third component of the spin (isospin) of i-th nucleon being s_i (τ_i) is expanded as follows:

$$\psi(\boldsymbol{r}) = \sum_{\alpha,m} 4\pi(1/2,s_1,1/2,s_2|S\mu)(1/2,\tau_1,1/2,\tau_2|T,T^3)(LmS\mu|JM)i^L Y^*_{L,m}(\hat{\boldsymbol{p}})\psi_\alpha(\boldsymbol{r}), \tag{29}$$

where the index α collectively denotes the quantum numbers of a partial wave; $\alpha = \{J,L,S,T\}$ where J,L,S are the total, orbital, total spin angular momenta of the NN system, respectively and T is the total isospin. The partial wave function (ψ_α) is expressed as

$$\psi_\alpha(\boldsymbol{r}) \;=\; \frac{1-(-1)^{L+S+T}}{\sqrt{2}}\sum_{L'}\mathcal{Y}_{L'SJ}(\hat{\boldsymbol{r}})\;R^J_{L',L;S}(r)\;\eta_{T,T^3}\;, \tag{30}$$

$$\mathcal{Y}_{LSJ}(\hat{\boldsymbol{r}}) \;=\; [Y_L(\hat{\boldsymbol{r}})\otimes\chi_S]_{(J)}\;, \tag{31}$$

where the two-nucleon spin (isospin) wave function is denoted by χ_S (η_T). The radial part of the above wave function is normalized, in the plane wave limit, to be

$$R^J_{L',L;S}(r) \to j_L(pr)\delta_{L,L'}. \tag{32}$$

With the multipole operators and the partial waves presented above, I express the transition amplitude in terms of the partial wave amplitudes:

$$\begin{aligned} T_{fi} \;=\; & \sum_{\alpha_i,m_i}\sum_{\alpha_f,m_f}\sum_{J_o,M_o}(-1)^{M_o}\; i^{J_o+L_i-L_f}\frac{(4\pi)^3}{\sqrt{2J_f+1}}Y^*_{L_i,m_i}(\hat{\boldsymbol{p}}_i)\; Y_{L_f,m_f}(\hat{\boldsymbol{p}}_f) \\ & \times(1/2,s_{1,i},1/2,s_{2,i}|S_i\mu_i)\;(1/2,\tau_{1,i},1/2,\tau_{2,i}|T_i,T_i^3)\;(L_im_iS_i\mu_i|J_iM_i) \\ & \times(1/2,s_{1,f},1/2,s_{2,f}|S_f\mu_f)\;(1/2,\tau_{1,f},1/2,\tau_{2,f}|T_f,T_f^3)\;(L_fm_fS_f\mu_f|J_fM_f) \\ & \times(J_iM_iJ_oM_o|J_fM_f)\sum_{a=C,L}\langle T_a^{J_o}\rangle\; Q_a^{J_o-M_o}\;, \end{aligned} \tag{33}$$

with the suffix i (f) indicates the initial (final) state. In the above equation, I used the abbreviation

$$\langle T_a^{J_o}\rangle \;=\; \langle\psi_{\alpha_f}||T_a^{J_o}||\psi_{\alpha_i}\rangle\;, \tag{34}$$

for the reduced matrix element defined by

$$\langle J_f,M_f|T_a^{J_o,M_o}|J_i,M_i\rangle = \frac{1}{\sqrt{2J_f+1}}(J_iM_iJ_oM_o|J_fM_f)\;\langle J_f||T_a^{J_o}||J_i\rangle\;. \tag{35}$$

B. Cross section

The unpolarized cross section for the $pp\to pn\pi^+$ reaction is

$$d\sigma = \sum_{\bar{i},f}\frac{1}{v_{rel}}\frac{1}{(2\pi)^5}\frac{1}{2\omega_\pi}\delta^{(4)}(P_i-q_\pi-P_f)|T_{fi}|^2 d\boldsymbol{q}_\pi d\boldsymbol{p}_{1,f}d\boldsymbol{p}_{2,f}\;, \tag{36}$$

where $\sum_{\bar{i},f}$ indicates the average (summation) over the initial (final) spin and isospin states of the two nucleons. The quantities P_i and P_f are the initial and final four total momentum of the two-nucleon system; $P_\mu^2=(P^0)^2-\boldsymbol{P}^2$. The relative velocity between the initial two nucleons is denoted by v_{rel}.

I derive the pion angular distribution, retaining only partial wave transition amplitudes of interest. I am primarily interested in the ${}^1S_0\to{}^3S_1$ transition amplitude, $\langle\psi_{^3S_1}||T_a^{J_o}||\psi_{^1S_0}\rangle$, where the $\tilde{d}$ term plays an important role. [It is noted that $\psi_{^3S_1}$ contains the ${}^3D_1$ component, as seen in Eq. (30), and thus the ${}^1S_0\to{}^3D_1$ transition is also included in $\langle\psi_{^3S_1}||T_a^{J_o}||\psi_{^1S_0}\rangle$.] However, I also retain the ${}^1D_2\to{}^3S_1$ transition amplitude for a later convenience. I retain

multipole operators with rank one ($J_o = 1$) which dominantly induce the transition. I integrate over the final two nucleon momenta to obtain:

$$\frac{d\sigma}{d\Omega_\pi} = \int_0^{q_\pi^{\max}} dq_\pi \; \frac{E_p \sqrt{q_\pi^2 + P_{f\,\mu}^2}\; p' q_\pi^2}{16\pi \; p \; \omega_\pi \; f_\pi^2} |M|^2 \; , \tag{37}$$

with

$$\begin{aligned} |M|^2 \; = \; & \frac{1}{4} \sum_{\alpha_i = {}^1S_0, {}^1D_2} |\langle \psi_{^3S_1} || T_C^1 - q_\pi T_L^1 || \psi_{\alpha_i} \rangle|^2 + P_2(\cos\theta_\pi) \left(\frac{1}{4} |\langle \psi_{^3S_1} || T_C^1 - q_\pi T_L^1 || \psi_{^1D_2} \rangle|^2 \right. \\ & \left. - \; \frac{1}{\sqrt{2}} \mathrm{Re} \left[\langle \psi_{^3S_1} || T_C^1 - q_\pi T_L^1 || \psi_{^1D_2} \rangle \langle \psi_{^3S_1} || T_C^1 - q_\pi T_L^1 || \psi_{^1S_0} \rangle^* \right] \right) \; . \end{aligned} \tag{38}$$

The scattering angle of the pion with respect to the direction of the initial proton is denoted by θ_π, and $P_2(x)$ is the Legendre function of degree two. The initial one nucleon energy is E_p and the maximum magnitude of the pion momentum is given by

$$q_\pi^{\max} = \frac{\sqrt{(E_p + m_N + m_\pi/2)(E_p + m_N - m_\pi/2)(E_p - m_N + m_\pi/2)(E_p - m_N - m_\pi/2)}}{E_p} \; . \tag{39}$$

I will compare my calculation with "partial wave amplitudes" extracted from experimental data in Ref. [11]. However, the "partial wave amplitudes" are actually different from the ordinary one, $\langle T_C^{J_o} - q_\pi T_L^{J_o} \rangle$. Therefore, I establish the relation between them so that the comparison makes sense, which will be done in the next paragraph.

In Ref. [11], six lowest partial wave amplitudes are assumed to contribute to the $pp \to pn\pi^+$ reaction in the energy region under investigation, and are extracted from the data. In extracting the amplitudes, they treated the final NN system as the "pseudo-deuteron" which is the NN scattering state with the relative motion integrated over; the pseudo-deuteron may have the angular momentum different from the deuteron. This means that they parameterized the data using a formulae in which the $pp \to pn\pi^+$ reaction was regarded as the $pp \to$ "d"π^+ reaction; "d" is the pseudo-deuteron. More specifically, they parameterized the pion angular distribution in the $pp \to pn\pi^+$ reaction using the formula:

$$\frac{d\sigma}{d\Omega_\pi} = C_0 + C_2 P_2(\cos\theta_\pi) \; , \tag{40}$$

with

$$C_0 \; = \; \frac{|a_0|^2}{4} + \frac{|a_1|^2}{4} + \frac{|a_2|^2}{4} + \frac{|b_0|^2}{4} + \frac{|b_1|^2}{4} + \frac{|b_2|^2}{4} \; , \tag{41}$$

$$C_2 \; = \; \frac{|a_2|^2}{4} - \frac{\mathrm{Re}[a_0 a_2^*]}{\sqrt{2}} \; , \tag{42}$$

where a_0 (a_2) is the partial wave amplitude for ${}^1S_0 \to {}^3S_1$ (${}^1D_2 \to {}^3S_1$); see Table IV of Ref. [11] for the other partial wave amplitudes. By comparing Eq. (40) with Eq. (37), I can

find the relation between the two differential cross section formula. To see the relation more clearly, I denote the theoretical counterpart to a_0 (a_2) by $\tilde{a}_0$ ($\tilde{a}_2$) and rewrite Eq. (37) as

$$\frac{d\sigma}{d\Omega_\pi} = \frac{|\tilde{a}_0|^2}{4} + \frac{|\tilde{a}_2|^2}{4} + \left(\frac{|\tilde{a}_2|^2}{4} - \frac{\mathrm{Re}[\tilde{\tilde{a}}_0 \tilde{\tilde{a}}_2^*]}{\sqrt{2}} \right) P_2(\cos\theta_\pi) \ , \tag{43}$$

with

$$|\tilde{a}_0|^2 = \int_0^{q_\pi^{\max}} dq_\pi \frac{E_p \sqrt{q_\pi^2 + P_{f\,\mu}^2}\, p' q_\pi^2}{16\pi\ p\ \omega_\pi\ f_\pi^2} |\langle \psi_{^3S_1} || T_C^1 - q_\pi T_L^1 || \psi_{^1S_0} \rangle|^2, \tag{44}$$

$$|\tilde{a}_2|^2 = \int_0^{q_\pi^{\max}} dq_\pi \frac{E_p \sqrt{q_\pi^2 + P_{f\,\mu}^2}\, p' q_\pi^2}{16\pi\ p\ \omega_\pi\ f_\pi^2} |\langle \psi_{^3S_1} || T_C^1 - q_\pi T_L^1 || \psi_{^1D_2} \rangle|^2, \tag{45}$$

$$\begin{aligned} \mathrm{Re}[\tilde{\tilde{a}}_0 \tilde{\tilde{a}}_2^*] &= \int_0^{q_\pi^{\max}} dq_\pi \frac{E_p \sqrt{q_\pi^2 + P_{f\,\mu}^2}\, p' q_\pi^2}{16\pi\ p\ \omega_\pi\ f_\pi^2} \\ &\times\ \mathrm{Re}\left[\langle \psi_{^3S_1} || T_C^1 - q_\pi T_L^1 || \psi_{^1D_2} \rangle \langle \psi_{^3S_1} || T_C^1 - q_\pi T_L^1 || \psi_{^1S_0} \rangle^* \right] \ . \end{aligned} \tag{46}$$

I distinctly used $\tilde{a}$ and $\tilde{\tilde{a}}$ because they are not necessarily the same.[10] Which ($\tilde{a}$ or $\tilde{\tilde{a}}$) should be compared with a_0 and a_2 from the experimental data ? I take the following way to find a solution.

At first, I factorize out the phase coming from the initial state interaction as

$$\tilde{a}_0 = e^{i\delta_0}\ \tilde{a}_0', \qquad \tilde{a}_2 = e^{i\delta_2}\ \tilde{a}_2' \ , \tag{47}$$

where δ_0 (δ_2) is the phase shift of the $^1S_0$ ($^1D_2$) partial wave scattering. I choose $\tilde{a}_0'$ and $\tilde{a}_2'$ to be real. The same factorization applies to $\tilde{\tilde{a}}_0$ and $\tilde{\tilde{a}}_2$. Then, as Step (i), I calculate $|\tilde{a}_0'|$ and $|\tilde{a}_2'|$ from Eq. (44) and Eq. (45), respectively. Next, as Step (ii), I solve a coupled equation consisting of Eq. (46) and $|\tilde{\tilde{a}}_0|^2 + |\tilde{\tilde{a}}_2|^2 = |\tilde{a}_0|^2 + |\tilde{a}_2|^2$ [the r.h.s. is from Step (i)], thereby finding a set of solutions, $\tilde{\tilde{a}}_0'$ and $\tilde{\tilde{a}}_2'$. Step (ii) is closer to the way how a_0 and a_2 are extracted from the data; each amplitude is extracted from the sum of the amplitudes (data). My numerical result shows that the two sets of the solutions obtained in Step (i) and (ii) are essentially the same in the absolute value. [Step (i) cannot fix the sign.][11] Therefore, I will employ the solution from Step (ii), in which the relative phase between $\tilde{a}_0$ and $\tilde{a}_2$ can also be fixed. (Hereafter, I do not distinguish between $\tilde{a}$ and $\tilde{\tilde{a}}$, and denote them by $\tilde{a}$.) Still, the overall phase of $\tilde{a}$ has not been fixed. In order to make the comparison with the data

[10] I use the symbol a ($\tilde{a}$) in a generic sense, referring to both a_0 and a_2 ($\tilde{a}_0$ and $\tilde{a}_2$).

[11] Strictly speaking, $\tilde{a}$ obtained in my analysis is not necessarily the same as a from Ref. [11]. In order to obtain a theoretically, one calculates the analyzing power and the pion angular distribution for the $pp \to pn\pi^+$ reaction, taking account of all non-negligible partial wave amplitudes. Then a is extracted from those observables in the same way as done in Ref. [11]. However, the fact that $\tilde{a}$ obtained in Step (i) and (ii) are essentially the same would indicate that my result would not change drastically even if I took the "ideal" procedure to calculate a.

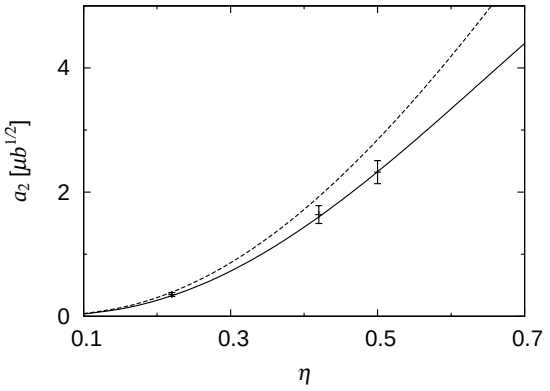

FIG. 2: The transition amplitude $\tilde{a}_2$ for $pp \to pn\pi^+$. The chiral NLO π production operator and the CD-Bonn NN potential are used. The solid curve is obtained with $h_A = 2.10$ while the dashed one with $h_A = 2.68$. Experimental data are from Ref. [11].

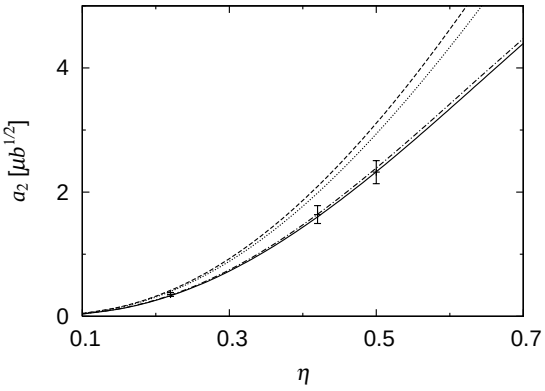

FIG. 3: The transition amplitude $\tilde{a}_2$ for $pp \to pn\pi^+$ obtained with the chiral NLO π production operator. I employ $h_A = 2.10$. The solid, dashed, dotted and dash-dotted curves are respectively $\tilde{a}_2$ obtained with the CD-Bonn, AV18, Reid93, Nijmegen I NN potentials. The result with the N^{3}LO potential almost exactly falls on the dash-dotted curve. Experimental data are from Ref. [11].

meaningful, one needs to choose the phase convention for $\tilde{a}$ to be the same as that for a. I use a_2 and $\tilde{a}_2$ to match the phase conventions of the experiment and the theory. I calculate $\tilde{a}_2$ using the same operator used in calculating $\tilde{a}_0$; the $\tilde{d}$ term does not contribute here. [12] I will fix the phase convention in this way in the next section, followed by the comparison between a_0 and $\tilde{a}_0$.

V. RESULT

A. $^1D_2 \to {}^3S_1$ transition amplitude

I calculate the $^1D_2 \to {}^3S_1$ transition amplitude, $\tilde{a}_2$, with the operators presented in Sec. II. Then, I compare $\tilde{a}_2$ with a_2 from the data[11]. In calculating $\tilde{a}_2$, I set the sharp cutoff $\Lambda = \infty$ because there is no counter term at this order which takes care of the high momentum components of the operators integrated out. In Fig. 2, I show $\tilde{a}_2$ obtained with the CD-Bonn NN potential, as a function of η ($\equiv q_\pi^{\rm max}/m_\pi$). As stated in Sec. III, I consider neither the Coulomb interaction nor isospin violation effects. I use the CD-Bonn

[12] Because of the finite cutoff, the $\tilde{d}$ term gives a very small contribution, which I safely neglect here.

potential for the proton-neutron channel. The solid curve is obtained with $h_A = 2.10$ (and the corresponding c_i's) while the dashed curve with $h_A = 2.68$. I choose the overall sign for $\tilde{a}_2$ such that a_2 and $\tilde{a}_2$ have the same sign, thereby fixing the phase convention. The phase convention does not change if I use a finite cutoff such as $\Lambda = 800$ MeV in calculating $\tilde{a}_2$. As observed in Fig. 2, $\tilde{a}_2$ with $h_A = 2.10$ falls exactly on the experimental data. We see the dependence of $\tilde{a}_2$ on the choice of the NN potential in Fig. 3. I used only $h_A = 2.10$ in Fig. 3. Although there is some dependence on the NN potential, all $\tilde{a}_2$ are on the vicinity of the data. χPT gives a successful description for a_2 at this order. Although a_2 is significantly larger than a_0 in magnitude, I stop the discussion on a_2 here and will give a detailed discussion on a_0 in the following subsections. This is because I am primarily concerned with the validity of the bridging program in this work, and a_0 is the one to be examined for this purpose.

B. $^1S_0 \to {}^3S_1$ transition amplitude

Now I move on to the $^1S_0 \to {}^3S_1$ transition amplitude, $\tilde{a}_0$. Because the relative phase between $\tilde{a}_2$ and $\tilde{a}_0$ is fixed within the theory, and the overall phase has been fixed by comparing a_2 and $\tilde{a}_2$, I am now able to compare a_0 and $\tilde{a}_0$ with the same phase convention. It is noted that my phase convention for $\tilde{a}_0$ is the same as the convention used in Ref. [5].

At first, in order to see the importance of the Δ, I mention a result obtained with the π-production operator without the Δ. I use the operators given in Eqs. (5), (10), (13)-(19) with the parameters taken from Ref. [8]. The cutoff function is also the same as that used in Ref. [8] (the Gaussian cutoff). I found a very large cutoff dependence of $\tilde{a}_0$ calculated with the Δ-less χPT. Depending on the cutoff ($\Lambda_\chi = 500$, 600 and 800 MeV), the contributions from the two-body operators to $\tilde{a}_0$ are different by a factor of 4, which demonstrates the failure of the Δ-less χPT in describing the p-wave π-production. I note that this result is quite different from the situation of the low-energy weak process where the Δ-less χPT gives the cross sections with a small cutoff dependence.

Next I present results obtained with the operator including the Δ. The operators have been presented in Sec. II, and the LEC $\tilde{d}$ has been fixed using the low-energy weak process in Sec. III. I am interested in how reasonably and reliably one can predict $\tilde{a}_0$ for the $pp \to pn\pi^+$ reaction using this χPT-based operator. For this purpose, I examine the dependence of $\tilde{a}_0$ on several inputs, Λ, h_A, $C_2^{N\Delta}$, and the NN potential. At first, in Fig. 4, I present a result obtained with the CD-Bonn NN potential and two choices of the h_A value. The partial wave amplitude $\tilde{a}_0$ is rather different from the experimental counterpart, a_0. For comparison, I also show a result obtained without the $\tilde{d}$ term. This result with $\tilde{d} = 0$ is similar to the case with $\delta = 0$ in Fig. 3 of Ref. [5] where a negative $\tilde{d}$ value (*e.g.*, $\delta = -0.2$) brings the theoretical amplitude into the agreement with the experimental one. In my calculation, however, the

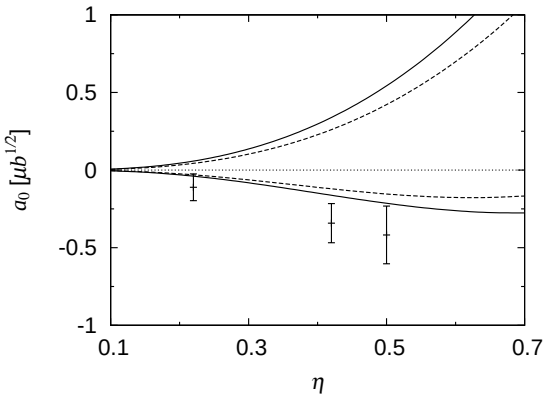

FIG. 4: The transition amplitude $\tilde{a}_0$ for $pp \to pn\pi^+$. The chiral NLO π production operator and the CD-Bonn NN potential are used. The solid and dashed curves correspond to $h_A = 2.10$ and 2.68, respectively; $\Lambda = 800$ MeV. The upper (lower) curves are obtained with (without) the $\tilde{d}$ term. Experimental data are from Ref. [11].

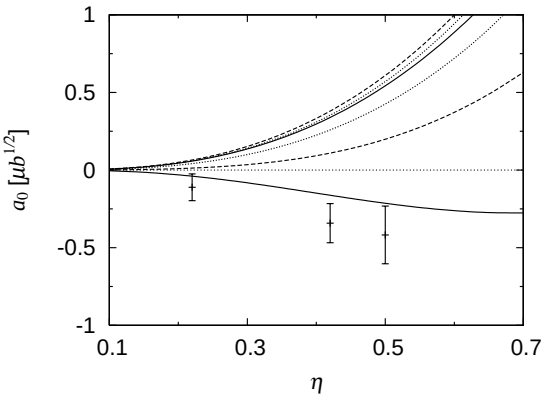

FIG. 5: The transition amplitude $\tilde{a}_0$ for $pp \to pn\pi^+$. The CD-Bonn NN potential is used. The solid, dashed and dotted curves correspond to Λ = 800, 600 and 500 MeV, respectively; h_A = 2.10. The upper (lower) three curves are obtained with (without) the $\tilde{d}$ term. Experimental data are from Ref. [11].

positive $\tilde{d}$ value (see the last row of the second and third columns in Table I) separates $\tilde{a}_0$ and a_0 furthermore; even the sign of $\tilde{d}$ fixed by the low-energy weak process is inconsistent with the experimental data of the π-production. I change the values of Λ and h_A and examine the dependence of $\tilde{a}_0$ on these inputs. The cutoff dependence is shown in Fig. 5. The situation of the disagreement does not change. [13] This result shows that the bridging program among reactions with quite different kinematics is not necessarily successful. This is understandable if we recall another case. For example, a chiral nuclear force[26, 29] describes the elastic NN scattering over a fairly wide energy region, partly because the LECs in it have been fixed using data from the same energy region. Therefore, it is no wonder to find that the operator fixed in the low-energy process cannot describe well the intermediate-energy process. In order to accurately describe the two reactions in the different energy regions simultaneously, data from both of the energy regions would be necessary to fix the LECs. It is also expected that higher order terms are necessary to accurately reproduce the data from the wide energy region, as in the case of the nuclear force.

We find from Fig. 5 the cutoff dependence ($\sim$10% level for $\tilde{a}_0$; the $\tilde{d}$ term included) which is much reduced compared with the Δ-less case. We also find a certain amount of dependence on the choice of h_A (Fig. 4), even if the $\tilde{d}$ value has been adjusted to eliminate the dependence

[13] For some combinations of h_A, Λ and NN potential, the sign of $\tilde{d}$ is consistent with the data. However, the strength is not enough to bring $\tilde{a}_0$ into agreement with a_0.

TABLE II: Contribution from each component of the operator to the matrix element for $pp \to d\pi^+$ (second row) and $pp \to de^-\nu_e$ (third row). Each contribution is divided by the "sum", and therefore, "1B" actually gives the matrix elements with the same sign for both cases. The CD-Bonn potential, $h_A = 2.10$, and $\Lambda = 800$ MeV are used. Some operators, not shown here, contribute to the π production by a small amount; at most, "WT" contributes by ~ 0.08.

kinematics	1B	$\Delta\pi$	ΔCT	c_3	c_4	$\tilde{d}$	sum (arb.units)
$pp \to d\pi^+$	-0.60	-0.54	0.97	-1.11	0.71	1.57	-0.0251
$pp \to de^-\nu_e$	0.996	0.009	-0.008	0.015	0.005	-0.017	0.757

on it at the low-energy kinematics. [14] This means that the Δ operator and the $\tilde{d}$ contact operator have quite different dependence on the kinematics, and it is important to take care of each component of the operator individually. The dependence on the kinematics is also found in Table II where I tabulated contributions from each component of the operator to $\tilde{a}_0$ for two kinematics; one for low-energy weak process ($pp \to de^-\nu_e$) where $\tilde{d}$ is fixed, and the other for the π-production ($pp \to d\pi^+$, $\eta = 0.5$). This situation is in contrast to the bridging program done in Ref. [8]. In Ref. [8], the operator fixed by a low-energy weak process (*i.e.*, the tritium β-decay) was used in another weak process which takes place in a relatively similar kinematics, and the result was given with a small cutoff dependence. I might say that it is not important to take care of each component of the operator individually in this case. Rather, one needs to take care of the sum of each component. This is also a reason why the pionless theory, whose two-body operator is just a contact operator, can reasonably describe several weak processes in a low-energy region[30].

From Table II, we also find that the contributions from the NLO operators is comparable to those from the LO operator. The LO contributions mostly cancel each other. For this reaction, there is no sign of the convergence in the chiral expansion up to this order. Furthermore, there is also a significant cancellation among the NLO contributions, which may make the amplitude sensitive to the higher order contributions. This situation reminds us of the result in Ref. [31, 32] where the $pp \to pp\pi^0$ reaction near threshold was studied with χPT. They found that some higher order two-pion-exchange mechanism contributes more than lower order one-pion-exchange mechanism, leading to a poor convergence of the chiral expansion. It would be important to do a higher order calculation of the p-wave π production to see the convergence of the chiral expansion.

We find in Table II that the contribution from the $\tilde{d}$ term is substantial. This result may

[14] The variation of h_A should be compensated for by the change of c_i and other higher order one-pion rescattering diagrams; not by the change of $\tilde{d}$. I will come back to this point later.

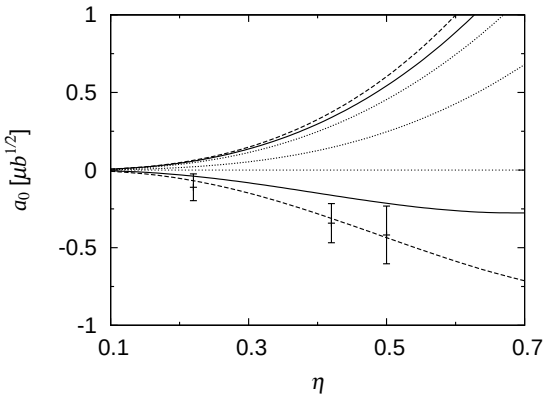

FIG. 6: The transition amplitude $\tilde{a}_0$ for $pp \to pn\pi^+$. The solid, dashed and dotted curves are respectively obtained with the CD-Bonn, AV18 and N^{3}LO NN potentials; $h_A = 2.10$ and $\Lambda = 800$ MeV. The upper (lower) three curves are obtained with (without) the $\tilde{d}$ term. Data are from Ref. [11].

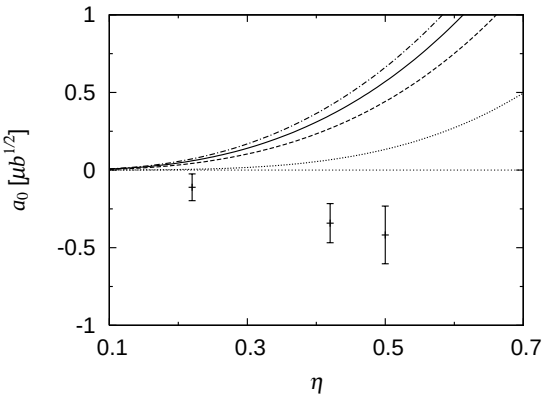

FIG. 7: The transition amplitude $\tilde{a}_0$ for $pp \to pn\pi^+$. The solid, dashed, dotted and dash-dotted curves are respectively obtained with the CD-Bonn, AV18, Reid93 and Nijmegen I NN potentials; $h_A = 2.10$ and $\Lambda = 500$ MeV. The N^{3}LO potential almost gives the solid curve. The $\tilde{d}$ term is included. Data are from Ref. [11].

also indicate the importance of a higher order calculation, which I will argue in the following. The large contribution from the $\tilde{d}$ term means that its dependence on the kinematics is rather influential on $\tilde{a}_0$. Because I am working at the NLO, two-pion-exchange (TPE) mechanisms are not explicitly considered but mimicked by the $\tilde{d}$ term. If the TPE and the $\tilde{d}$ term have rather different dependence on the kinematics, $\tilde{a}_0$ given by the NLO and NNLO calculations may be significantly different.

I show results obtained with various NN potentials to see the dependence of $\tilde{a}_0$ on it. The result is shown in Fig. 6. We find a considerable dependence on the NN potential, even though all NN potentials give almost the same amplitude in the low-energy region where the $\tilde{d}$ value has been fixed. The $\tilde{d}$ term is quite sensitive to the short-distance behavior of the wave function because of its point-like nature. Therefore, when the cutoff is relatively large and thus the short-distance behavior of the wave function is very dependent on the NN potential, the $\tilde{d}$ value is also largely dependent on the NN potential. In case of $\Lambda = 800$ MeV, for example, a part of the dependence of $\tilde{a}_0$ on the NN potential is ascribable to that the $\tilde{d}$ term alone is too simple to compensate for the difference in the short distance physics. However, I consider that there is a more influential source of the dependence on the NN potential, because we still find the dependence in the case of $\Lambda = 500$ MeV (Fig. 7). Let me explain more on this in the following. In the rest of this paragraph, I discuss the case with $\Lambda = 500$ MeV. At this cutoff, the details of the short distance physics have been integrated out substantially, and therefore there is no significant difference among the wave functions

for different NN potentials any more. Recall that low-momentum NN potentials obtained from various phenomenological NN potentials are very similar at $\Lambda \sim 400$ MeV[33, 34]. In this situation, the $\tilde{d}$ values for different NN potentials should be almost the same to give almost the same $\tilde{a}_0$. Contrary to this expectation, I obtained quite different $\tilde{d}$ as seen in the second row of TABLE I, leading to rather different $\tilde{a}_0$. [15] I suspect that the $\tilde{d}$ term alone is too simple to simulate the operator *to be simulated*, [16] and that my procedure of determining $\tilde{d}$, discussed in the previous section, gives the $\tilde{d}$ term which is far from being as approximate to the operator *to be simulated* as it can be. I suspect that this is the main source of the NN dependence of $\tilde{a}_0$. The relatively large h_A-dependence of $\tilde{d}$ (and $\tilde{a}_0$) is also likely to have the same origin. In order to improve the situation, one would need to do a higher order calculation, and include a few more contact operators so that a better simulation can be done. [17]

Because I treated the contact $NN \to N\Delta$ interaction in the phenomenological manner, as discussed in Sec. II, it is informative to study an impact of changing the coupling on the amplitude $\tilde{a}_0$. For this purpose, I change the $C_2^{N\Delta}$ value by $\pm$ 10%, re-fit the $\tilde{d}$ value in the way discussed in Sec. III, and calculate $\tilde{a}_0$. I found that $\tilde{a}_0$ is less dependent on the variation of $C_2^{N\Delta}$ than that of h_A. This result may be understood as follows. The contact-induced Δ-excitation mechanism [Fig. 1(c)] is similar to the $\tilde{d}$ term [Fig. 1(e)] in the sense that Fig. 1(c) is reduced to Fig. 1(e) in the Δ-less theory. Therefore, one may expect that the variation of $C_2^{N\Delta}$ is fairly well compensated for by the change of $\tilde{d}$.

C. $^1S_0 \to {}^3S_1$ transition amplitude with one more counter term

As seen in the previous section, the bridging program was not successful; the χPT-based operator with $\hat{d}(\equiv m_N f_\pi^2 \tilde{d})$ fixed by the low-energy weak process does not reproduce the partial wave amplitude for the π-production, a_0, extracted from the data. Because I have pointed out several reasons for expecting a higher order calculation, here I try to see what happens there by doing a simple extension of my calculation. The extension is to add a

[15] In the next subsection where I include one more contact term, we will see that the expectation is realized.

[16] Even though we do not know, there should exist an operator which the $\tilde{d}$ term tries to simulate. The operator should include all non-negligible chiral operators other than those explicitly considered already. I refer to the operator as the operator *to be simulated*.

[17] One might suspect that the dependence on the NN potential is due to a difference in the phase shift of the $^1S_0$ partial wave in the energy region above the pion production threshold. Among the NN potentials I use, the phase shifts from the Reid93 and the N^{3}LO potentials are noticeably different from the others at this energy. However, I do not consider the difference in the phase shift to be influential because the inclusion of one more contact term results in that all of the NN potentials with $\Lambda = 500$ MeV give essentially the same $\tilde{a}_0$ over the entire energy region under consideration. Note that the contact term does not reflect the difference in the long range behavior (phase shift) of the wave function.

TABLE III: Dimensionless contact couplings, $\hat{d}$ and $\hat{e}$. The first column is the sharp cutoff value, and the others are values of the LECs. The 2–4th rows are for the $\hat{d}$ values while 5–7th rows for the $\hat{e}$ values. For each NN potential, the left side is the LECs for $h_A = 2.10$ while the right side for $h_A = 2.68$.

Λ	CD-Bonn		AV18		Reid93		Nij I		N^{3}LO	
500	0.57	0.57	0.45	0.46	0.43	0.44	0.51	0.51	−0.22	−0.21
600	0.49	0.48	0.20	0.19	0.15	0.14	0.37	0.36	−4.12	−4.08
800	−1.15	−1.34	3.06	3.30	3.12	3.35	−5.41	−6.14	8.42	8.35
500	0.85	0.85	0.94	0.94	0.96	0.95	0.90	0.90	1.44	1.43
600	1.10	1.11	1.35	1.36	1.40	1.41	1.20	1.22	5.15	5.12
800	3.39	3.60	−1.55	−1.84	−1.62	−1.89	8.38	9.23	−7.83	−7.75

higher order counter term to the NLO χPT-based operator used in the previous section. I use the following counter term of $\mathcal{O}[(m_\pi/m_N)^2]$ [18]:

$$\mathcal{L}^{(2)}_{\rm CT} = -\frac{\hat{e}}{m_N f_\pi^2 \Lambda^2} N^\dagger \boldsymbol{\tau} \cdot \vec{\sigma} \cdot \vec{\nabla} \boldsymbol{\pi} N \left(N^\dagger \vec{\nabla}^2 N + \text{h.c.} \right) , \tag{48}$$

where the dimensionless LEC is denoted by $\hat{e}$. This is not a general form of the counter terms at this order, and there are other counter terms with different spin-isospin and derivative structures. However, it is sufficient to consider only this counter term for my purpose of gaining a rough insight into a higher order calculation.

Now I have the two independent LECs: $\hat{d}$ and $\hat{e}$. I fix these two LECs so that the following two conditions are satisfied. The first condition is the same as that used in Sec. III for fixing $\hat{d}$. This condition is from the low-energy weak process. The second condition is due to a_0 extracted from the experimental data for the $pp \to pn\pi^+$ reaction[11]. I choose the LECs so that the central value of the empirical amplitude, $a_0(\eta = 0.5) = -0.418\ \mu\text{b}^{1/2}$, is reproduced. As seen in the previous section, one cannot reproduce the π-production partial wave amplitude (a_0) by using $\hat{d}$ fitted to the amplitude of the low-energy weak process alone. The disagreement between a_0 and $\tilde{a}_0$ is rather serious; even the sign of $\hat{d}$ is inconsistent with the data in some cases. Therefore, it is not obviously expected that the addition of the $\hat{e}$ term with a *natural* strength brings $\tilde{a}_0$ into agreement with a_0. However, such a set of $\hat{d}$ and $\hat{e}$ does exist, as presented in Table III.

[18] There exist $\mathcal{O}[(m_\pi/m_N)^{3/2}]$ operators coming from pion-loop diagrams. For a simple analysis, I use the $\mathcal{O}[(m_\pi/m_N)^2]$ counter term.

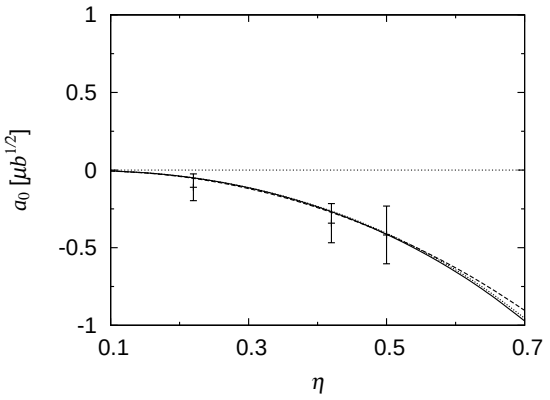

FIG. 8: The transition amplitude $\tilde{a}_0$ for $pp \to pn\pi^+$. The chiral NLO π production operator plus the counter term [Eq. (48)] and the CD-Bonn NN potential are used. The solid, dashed and dotted curves correspond to $\Lambda = 800$, 600 and 500 MeV, respectively, and $h_A = 2.10$. Experimental data are from Ref. [11].

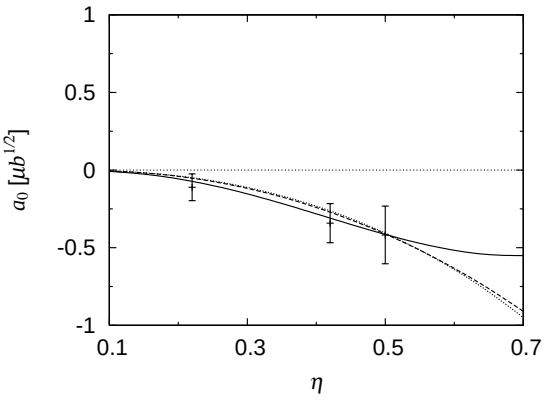

FIG. 9: The transition amplitude $\tilde{a}_0$ for $pp \to pn\pi^+$. The AV18 NN potential is used. The other features are the same as Fig. 8.

I calculate $\tilde{a}_0$ with the parameter sets in Table III. The results for the CD-Bonn and the AV18 NN potentials are shown in Figs. 8 and 9, respectively. I show results obtained with $h_A = 2.10$ only. The dependence of $\tilde{a}_0$ on h_A is small in this case. By construction, the calculated $\tilde{a}_0$ goes through the central value of the data at $\eta = 0.5$. The η dependence of $\tilde{a}_0$ is consistent with the data for all NN potentials and for all Λ. Particularly, all NN potentials give essentially the same $\tilde{a}_0$ for $\Lambda = 500$ MeV. From Table III, we also observe that the couplings $\hat{d}$ and $\hat{e}$ for $\Lambda = 500$ MeV are similar for all the NN potentials, except for the N^{3}LO potential. In fact, this result has been expected; see footnote 15. For $\Lambda = 800$ MeV, a relatively large dependence of $\tilde{a}_0$ (two types of the behavior) on the NN potential is observed, within the consistency with the data. Regarding the CD-Bonn and the Nijmegen I potentials, $\tilde{a}_0$ ($\Lambda = 800$ MeV) is very similar to $\tilde{a}_0$ ($\Lambda = 500$ or 600 MeV); see Fig. 8. On the other hand, the other NN potentials give $\tilde{a}_0$ ($\Lambda = 800$ MeV) whose η-dependence is quite different from $\tilde{a}_0$ ($\Lambda = 500$ or 600 MeV); see Fig. 9. From a viewpoint of the renormalization group, the operators with $\Lambda = 500$, 600 and 800 MeV should be related by integrating out the high momentum states whose effects are simulated by the renormalization of $\hat{d}$ and $\hat{e}$. If this relation is realized, these operators should give the same observables, to the extent that the contact operators simulate the high energy modes integrated out. From this viewpoint, the results for the CD-Bonn (Fig. 8) and the Nijmegen I are understandable, while the others (Fig. 9) are not. However, the situation may change in a correct higher order calculation where the TPE is explicitly considered. This is because the model space

employed here probably has a resolution at which the contact operators cannot accurately simulate the intermediate-range mechanism such as TPE. If the TPE is explicitly considered, then the contact operators do not have to mimic the intermediate-range mechanism, and more accurately describe the shorter-range mechanism.

I look into the contact operators for different NN potentials, and understand the similar (different) η-dependence of $\tilde{a}_0$ for $\Lambda = 500$ (800) MeV among different NN potentials. As representatives, I show the contact operators for the CD-Bonn and the AV18 potentials in Figs. 10 and 11, respectively. We can find that the contact operators, including both $\hat{d}$ and $\hat{e}$, for $\Lambda = 500$ (800) MeV are very similar (different), leading to the quite similar (different) η dependence of $\tilde{a}_0$. Starting with the operators for $\Lambda = 800$ MeV, one can reduce Λ to examine the running of the operators using the Wilsonian RG equation. I refer the readers to Refs. [35, 36] for a detailed explanation of how I reduce Λ, and just show the result here. In Fig. 12, the RG running of the contact operator for the CD-Bonn potential is given. For a comparison, the contact operator for $\Lambda = 500$ MeV, whose LECs are given in Table III, are also shown. We can see that the contact operators ($\Lambda = 500$ MeV) derived in the different two ways, one from directly fitting to the data and the other from the RG running, are fairly similar. Although the figure shows the result for the diagonal components of the operators, the same level of the agreement is confirmed for off-diagonal components. For the AV18 potential, however, the two contact operators ($\Lambda = 500$ MeV) with the different origins are quite different as shown in Fig. 13. This result has been expected by observing Fig. 9 where the contact operators with $\Lambda = 500$ and 800 MeV do not give the same result, indicating that the two operators are not equivalent.

I compare the contact operator including both $\hat{d}$ and $\hat{e}$ (Table III), and those with only $\hat{d}$ (Table I) in Figs. 10 and 11. A naive expectation is that a contact operator with $\hat{d}$ only (a dashed curve) is an approximation of the one with $\hat{d}$ and $\hat{e}$ (the solid curve). In the two figures, this expectation is not always the case, and therefore we have to be careful about the convergence of the chiral expansion of the short distance physics. In any case, the $\hat{d}$ term alone cannot be a good approximation of the $\hat{d}$ plus $\hat{e}$ terms and, for that matter, not a good approximation of the operator *to be simulated*. It is recalled that this observation has been used in the previous subsection to argue over a reason for the dependence of $\tilde{a}_0$ on h_A and the NN potential. By including the $\hat{e}$ term, the situation is much improved in this point. We found the very small dependence of $\tilde{a}_0$ on the choice of h_A and on the NN potential for $\Lambda = 500$ MeV. Regarding the $\hat{d}$ and $\hat{e}$ values, as seen in Table III, they hardly depend on h_A. This is quite consistent with the discussion given in footnote 14.

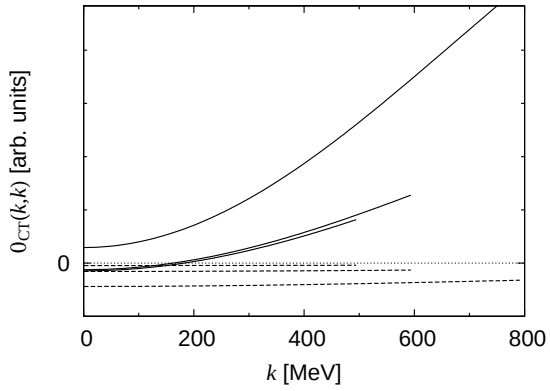

FIG. 10: The contact operators for the CD-Bonn potential. The diagonal components in the momentum space are given. The solid curves are parameterized by both $\hat{d}$ and $\hat{e}$, while the dashed curves by $\hat{d}$ only. The k-coordinate value at the end point of a curve indicates the value of Λ for the operator. $h_A = 2.10$.

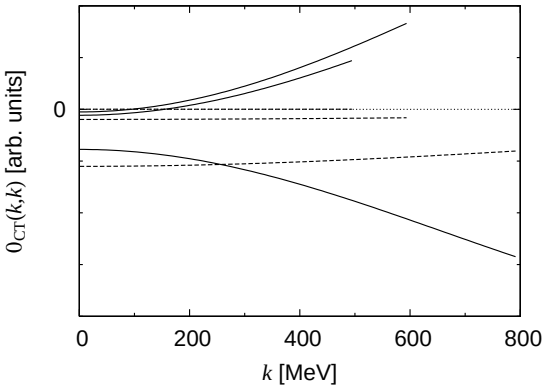

FIG. 11: The contact operators for the AV18 potential. The other features are the same as Fig. 10. The scale is also the same as Fig. 10.

VI. SUMMARY

I determined the LEC $\hat{d}$ using the low-energy weak process and then used it to predict the partial wave amplitude, $\tilde{a}_0$ ($^1S_0 \to {}^3S_1$), for the $pp \to pn\pi^+$ reaction. Through this work, I tried to explore the power of χPT that enables one to bridge different reactions. My investigation is more stringent test of this aspect of χPT than similar analyses in the literature because the reactions connected through χPT here take place under significantly different kinematics.

I started with the chiral Lagrangian including the nucleon, pion and Δ. It is mandatory to include the Δ explicitly for describing the p-wave π production. With the Lagrangian, I constructed, up to NLO of the chiral expansion proposed in Ref. [5, 13], a set of operators which describes the Gamow-Teller transition in low-energy weak processes and the p-wave π-production. I fixed the remaining unknown LEC $\hat{d}$ (indirectly) using the experimental data of the low-energy weak process. Then I calculated the partial wave amplitudes ($\tilde{a}$) for the $pp \to pn\pi^+$ reaction. I chose the phase convention such that $\tilde{a}_2$ ($^1D_2 \to {}^3S_1$) has the same phase as a_2 extracted from the data in Ref. [11]. My prediction of $\tilde{a}_0$ using the NLO operator does not agree with the data. I used several different sets of the inputs such as the NN potential, h_A and Λ. Even though there is some dependence of $\tilde{a}_0$ on these inputs, all results differ from the data in the similar manner. Unfortunately, even the sign of $\hat{d}$, fixed by the weak process, is sometimes not consistent with the data. This result indicates that the

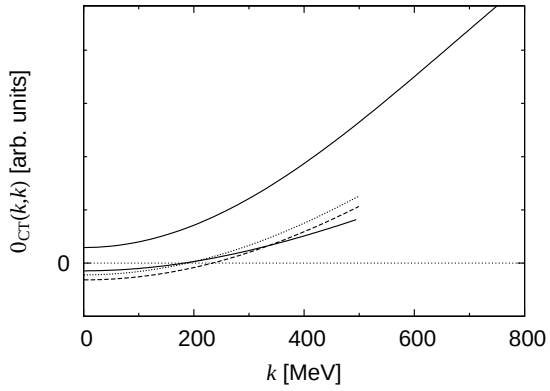

FIG. 12: RG running of contact operators for the CD-Bonn potential. The solid curves are the same as those in Fig. 10. (The curve for $\Lambda = 600$ MeV is not shown.) The dashed and dotted curves are derived from the solid curve for $\Lambda = 800$ MeV by solving the RG equation. The dashed (dotted) curve is obtained with the kinematics for the $pp \to d\pi^+$ ($pp \to de^+\nu_e$) reaction.

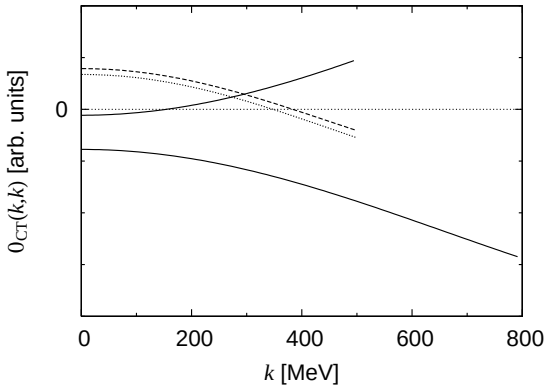

FIG. 13: RG running of contact operators for the AV18 potential. The solid curves are the same as those in Fig. 11. The other features are the same as Fig. 12.

bridging program between the two reactions with quite different kinematics is not always successful. In the literature, we have sometimes found an argument which supposes that the bridging program works. Given the result here, it is clear that we need to seriously study a feasibility of the bridging program, particularly for reactions with different kinematics. This conclusion may be disappointing, but still understandable if we recall the success of the chiral nuclear force. The chiral nuclear force accurately describes the NN scattering over a wide energy region, partly because the LECs included have been fixed using data from the same energy region. In fact, there are several reasons to expect a higher order calculation to significantly improve the situation. First of all, one may naively think that the NLO, tree level, operator is too simple to describe the π production. We know that two-pion-exchange mechanism and higher order contact terms are necessary for accurately describing the NN elastic scattering near the π production threshold. Second, the $\hat{d}$ term largely contributes to $\tilde{a}_0$, and therefore it would be important to extract the TPE mechanism from the $\hat{d}$ term, thereby describing the intermediate-range mechanism more elaborately and reducing the role of the $\hat{d}$ term. Third, $\tilde{a}_0$ is considerably dependent on the choice of the NN potential, which means that the single contact term is too simple to cancel out different short distance physics for different NN potentials. I also argued that a substantial part of the NN-dependence (and h_A-dependence) of $\tilde{a}_0$ is likely to be ascribable to the fact that

the $\hat{d}$ term alone is too simple to simulate the operator *to be simulated*. Meanwhile, a higher order calculation is also desirable to see the convergence of the chiral expansion; regarding the $pp \to pn\pi^+$ reaction, we found no sign of the convergence up to this order.

In order to explore, even roughly, a result of a higher order calculation, I added a higher order counter term, with the LEC $\hat{e}$, to the NLO operator. I fitted the LECs $\hat{d}$ and $\hat{e}$ to both the Gamow-Teller amplitude for the low-energy weak process and $\tilde{a}_0$ for the π production. I found a set of the LECs with the natural strength. The LECs are mostly independent of the choice of h_A as they should; without the $\hat{e}$ term, however, $\hat{d}$ is rather dependent on h_A. With this parameter set, η-dependence of $\tilde{a}_0$ is described in a way consistent with experimental data, irrespective of the choices of the NN potential, h_A and Λ. This result would be an indication that a higher order calculation is promising. I found that the single $\hat{d}$ term is not always a good approximation of the $\hat{d}$ plus $\hat{e}$ terms. I also showed using the RG analysis that the contact operators with different cutoff are not always equivalent. These findings tell us to be careful about the convergence of the chiral expansion, and also the importance of going to a higher order calculation.

Acknowledgments

I acknowledge B. K. Jennings for reading the manuscript and comments. I also thank C. Hanhart and D. R. Phillips for useful discussions. The Natural Sciences and Engineering Research Council of Canada is thanked for financial support. TRIUMF receives federal funding via a contribution agreement through the National Research Council of Canada.

APPENDIX A: MULTIPOLE EXPANSION OF $O_{\Delta\pi}$ OPERATOR

I present our calculational procedure for the $O_{\Delta\pi}$ operator [Eq. (6)]. I start with the Fourier transform of $O_{\Delta\pi}$:

$$\int \frac{dk^3}{(2\pi)^3} e^{-i\boldsymbol{k}\cdot\boldsymbol{r}} \frac{\boldsymbol{k}\,\boldsymbol{\sigma}_2\cdot\boldsymbol{k}}{m_\pi^{\prime 2}+k^2} \frac{f(k)}{m_\Delta - m_N - p_o^2/m_N + (\boldsymbol{p}'+\boldsymbol{q}_\pi/2)^2/2\mu} , \tag{A1}$$

where I only consider one term in $O_{\Delta\pi}$; the other terms and a constant factor are omitted. The function $f(k)$ is a cutoff function: $f(k) = \exp\left(-k^2/\Lambda_G^2\right)$ with $\Lambda_G = 2$ GeV. In this equation, I expand the energy denominator as follows:

$$\begin{aligned} D(\boldsymbol{p}', \boldsymbol{q}_\pi) &= \frac{1}{m_\Delta - m_N - p_o^2/m_N + (\boldsymbol{p}'+\boldsymbol{q}_\pi/2)^2/2\mu} \\ &= 4\pi \sum_\ell (-1)^\ell \sqrt{2\ell+1}\, [Y_\ell(\hat{\boldsymbol{p}}') \otimes Y_\ell(\hat{\boldsymbol{q}}_\pi)]^0_{(0)}\, D_\ell(p', q_\pi) , \end{aligned} \tag{A2}$$

where $D_\ell(p', q_\pi)$ is defined by

$$\begin{aligned} D_\ell(p', q_\pi) &= \frac{1}{2}\int_{-1}^{1} D(\boldsymbol{p}', \boldsymbol{q}_\pi) P_\ell(z) dz \\ &= \frac{1}{2}\int_{-1}^{1} \frac{P_\ell(z) dz}{(p' q_\pi/2\mu)(\beta + z)} \\ &= \frac{(-1)^\ell}{(p' q_\pi/2\mu)} Q_\ell(\beta) \ , \end{aligned} \tag{A3}$$

with

$$\beta \equiv \frac{m_\Delta - m_N - p_o^2/m_N + (p'^2 + q_\pi^2/4)/2\mu}{p' q_\pi/2\mu} \ , \tag{A4}$$

and $z \equiv \hat{\boldsymbol{p}}' \cdot \hat{\boldsymbol{q}}_\pi$. The function $Q_\ell(\beta)$ is the Legendre function of the second kind, and is given by

$$Q_\ell(\beta) = \frac{1}{2}\int_{-1}^{1} \frac{P_\ell(z) dz}{\beta - z} \ . \tag{A5}$$

I write Eq. (A1) using the expanded form Eq. (A2). When I retain only the first term ($\ell = 0$) of the expansion, I obtain

$$\begin{aligned} & \int \frac{dk^3}{(2\pi)^3} e^{-i\boldsymbol{k}\cdot\boldsymbol{r}} \frac{\boldsymbol{k}\ \boldsymbol{\sigma}_2 \cdot \boldsymbol{k}}{m_\pi'^2 + k^2} \ \frac{2\mu}{p' q_\pi} Q_0(\beta) f(k) \\ &= \left(\frac{1}{3}\boldsymbol{\sigma}_2 F_0(r) + \frac{\sqrt{8\pi}}{3} \left[Y_2(\hat{\boldsymbol{r}}) \otimes \boldsymbol{\sigma}_2 \right]_{(1)} F_2(r) \right) \frac{2\mu}{p' q_\pi} Q_0(\beta) \ , \end{aligned} \tag{A6}$$

with

$$\begin{aligned} F_0(r) &= \frac{1}{2\pi^2}\int_0^\infty dk \frac{k^4}{k^2 + m_\pi'^2} j_0(kr) f(k) \ , \\ F_2(r) &= \frac{1}{2\pi^2}\int_0^\infty dk \frac{k^4}{k^2 + m_\pi'^2} j_2(kr) f(k) \ . \end{aligned} \tag{A7}$$

I take a matrix element of Eq. (A1) after setting $q_\pi = 0$, and compared it with the matrix element of Eq. (A6) in which $q_\pi (\neq 0)$ is fixed by the kinematics. In the kinematical region of interest, I found a small correction ($\sim 1.5\%$). The use of Eq. (A6) may be regarded as an inclusion of the lowest order correction [$\mathcal{O}(q_\pi^2)$] from finite q_π, even though there is still another $\mathcal{O}(q_\pi^2)$ correction. I do not consider the higher order ($\ell \geq 1$) terms in Eq. (A2) to be influential on our result because: the $\mathcal{O}(q_\pi^2)$ correction from Eq. (A6) is small; the expansion in Eq. (A2) may be regarded as an expansion in terms of z/β, and $z/\beta \ll 1$ in most of the kinematical region of interest. I use Eq. (A6) in our calculation.

---

[1] S. R. Beane, P. F. Bedaque, W. C. Haxton, D. R. Phillips and M. J. Savage, in *At the frontier of particle physics*, edited by M. Shifman (World Scientific, 2001), vol. 1, p. 133;

nucl-th/0008064; P. Bedaque and U. van Kolck, Annu. Rev. Nucl. Part. Sci. **52**, 339 (2002); E. Epelbaum, Prog. Part. Nucl. Phys. **57**, 654 (2006).

[2] C. Hanhart, Phys. Rep. **397**, 155 (2004).

[3] K. Kubodera and T.-S. Park, Annu. Rev. Nucl. Part. Sci. **54**, 19 (2004).

[4] D. Hüber, J. L. Friar, A. Nogga, H. Witała and U. van Kolck, Few-Body Systems **30**, 95 (2001).

[5] C. Hanhart, U. van Kolck and G. A. Miller, Phys. Rev. Lett. **85**, 2905 (2000).

[6] A. Gårdestig and D. R. Phillips, Phys. Rev. Lett. **96**, 232301 (2006).

[7] A. Gårdestig and D. R. Phillips, Phys. Rev. C **73**, 014002 (2006); A. Gårdestig, Phys. Rev. C **74**, 017001 (2006).

[8] T.-S. Park, L. E. Marcucci, R. Schiavilla, M. Viviani, A. Kievsky, S. Rosati, K. Kubodera, D.-P. Min and M. Rho, Phys. Rev. C **67**, 055206 (2003).

[9] S. Ando, Y. H. Song, T.-S. Park, H.W. Fearing and K. Kubodera, Phys. Lett. **B555**, 49 (2003).

[10] S. Ando, T.-S. Park, K. Kubodera and F. Myhrer, Phys. Lett. **B533**, 25 (2002).

[11] R. W. Flammang *et al.* , Phys. Rev. C **58**, 916 (1998).

[12] J. Haidenbauer, K. Holinde and M. B. Johnson, Phys. Rev. C **48**, 2190 (1993).

[13] T. D. Cohen, J. L. Friar, G. A. Miller, and U. van Kolck, Phys. Rev. C **53**, 2661 (1996).

[14] S. Weinberg, Phys. Lett. **B251**, 288 (1990); Nucl. Phys. **B363**, 3 (1991).

[15] C. Ordóñez, L. Ray and U. van Kolck, Phys. Rev. C **53**, 2086 (1996).

[16] H. Krebs, E. Epelbaum and U.-G. Meißner, Eur. Phys. J. A **32**, 127 (2007).

[17] T. R. Hemmert, B. R. Holstein and J. Kambor, J. Phys. G **24**, 1831 (1998).

[18] E. Matsinos, Phys. Rev. C **56**, 3014 (1997).

[19] R. Schiavilla, V. G. J. Stoks, W. Glöckle, H. Kamada, A. Nogga, J. Carlson, R. Machleidt, V. R. Pandharipande, R. B. Wiringa, A. Kievsky, S. Rosati and M. Viviani, Phys. Rev. C **58**, 1263 (1998).

[20] A. Gårdestig, D. R. Phillips and Ch. Elster, Phys. Rev. C **73**, 024002 (2006).

[21] V. Lensky, V. Baru, J. Haidenbauer, C. Hanhart, A. E. Kudryavtsev, and U.-G. Meißner, Eur. Phys. J. A **27**, 37 (2006).

[22] R. B. Wiringa, V. G. J. Stoks, and R. Schiavilla, Phys. Rev. C **51**, 38 (1995).

[23] B. S. Pudliner, V. R. Pandharipande, J. Carlson and R. B. Wiringa, Phys. Rev. Lett. **74**, 4396 (1995).

[24] R. Machleidt, Phys. Rev. C **63**, 024001 (2001).

[25] V. G. J. Stoks, R. A. M. Klomp, C. P. F. Terheggen and J. J. de Swart, Phys. Rev. C **49**, 2950 (1994).

[26] D. R. Entem and R. Machleidt, Phys. Rev. C **68**, 041001(R) (2003).

[27] S. X. Nakamura, Prog. Theor. Phys. **114**, 713 (2005).

[28] J. D. Walecka, in *Muon Physics*, edited by V. W. Hughes and C. S. Wu (Academic, New York, 1975), Vol. 2, p. 113.

[29] E. Epelbaum, W. Glöckle, Ulf-G. Meißner Nucl. Phys. **A747**, 362 (2005).

[30] M. Butler and J.-W. Chen, Phys. Lett. **B520**, 87 (2001); M. Butler, J.-W. Chen and X. Kong, Phys. Rev. C **63**, 035501 (2001); J.-W. Chen, G. Rupak and M. J. Savage, Nucl. Phys. **A653**, 386 (1999).

[31] S. Ando, T.-S. Park and D.-P. Min, Phys. Lett. **B509**, 253 (2001).

[32] Y. Kim, T. Sato, F. Myhrer and K. Kubodera, Phys. Lett. **B657**, 187 (2007).

[33] S. Bogner, T. T. S. Kuo, and L. Coraggio, Nucl. Phys. **A684**, 432 (2001); S. K. Bogner, T. T. S. Kuo, and A. Schwenk, Phys. Rep. **386**, 1 (2003).

[34] S. X. Nakamura, Prog. Theor. Phys. **114**, 77 (2005).

[35] S. X. Nakamura and S. Ando, Phys. Rev. C **74**, 034004 (2006).

[36] S. X. Nakamura and A. Gårdestig, arXiv:0704.3757.